Self-Retractable Soft Growing Robots for Reliable and Fast Retraction While Preserving Their Inherent Advantages

Nam Gyun Kim[1], Dongoh Seo[1], Shinwoo Park[2] and Jee-Hwan Ryu[2]

***Abstract*— Soft growing robots have garnered significant research interest owing to their unique locomotion. However, real-world applications of these robots are limited by challenges in achieving reversible and repeatable operations, particularly when faced with buckling during retraction. Although a variety of retraction mechanisms have been developed, many necessitate the installation of extra rigid hardware at the distal part, compromising the inherent benefits of soft growing robots. Existing soft retraction mechanisms that maintain these advantages tend to be relatively slow and rely on heavy driving fluids. This study introduces a soft retraction mechanism that depends exclusively on the existing pneumatic force, eliminating the need for additional rigid hardware, power sources, or complex control procedures. This mechanism enables rapid and reliable retraction of soft growing robots without sacrificing their inherent advantages or interfering with their inner channels during retraction. The proposed mechanism's straightforward structure facilitates easy integration with a wide range of tip mounts, steering mechanisms, and other application-specific soft growing robots. This research offers an analysis and experimental examination of the operating principles and behaviors of the proposed mechanism. It also presents the design guidelines and fabrication details for the mechanism, as well as a demonstration of its swift and buckling-free retraction. In summary, the proposed retraction mechanism holds the potential to significantly improve practical applications of soft growing robots.**

I. Introduction

Soft growing robots have gained prominence in soft robotics research due to their exceptional locomotion capabilities that surpass traditional robots [1]. Also known as "vine robots" [2], they can extend their bodies unhindered by the environment. This feature enables them to navigate confined spaces with openings smaller than their width, and continue growing even when punctured, owing to their pneumatically driven design. Moreover, their frictionless growth enables exploration of slippery or sticky terrain, climbing high walls, and traversing cliffs.

Ongoing research aims to enhance the performance of soft growing robots, broadening their applications. They have been utilized for search and rescue operations, navigating tight spaces and rubble to locate and save victims [3]. Additionally, they have been employed to explore caves [4], coral reefs [5], and collapsed buildings [6], as they can adapt to confined spaces' shapes and move through them without causing damage. In medical applications, their shape-morphing property and frictionless growth mechanism enable safe movement around organs. Soft growing catheters have been designed to reduce force on the human body [7], whereas miniature soft growing robots have been developed to detect invasive cancer precursors using an internal steering mechanism with a soft catheter [8].

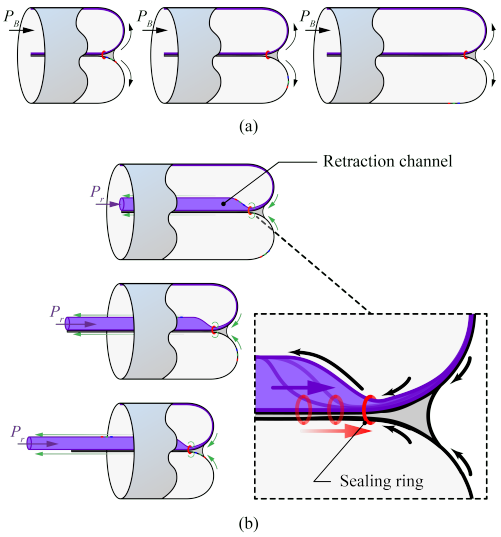

Fig. 1. Schematic of self-retractable (SR) mechanism. (a) Forward operation of the soft growing robot with SR mechanism. (b) Retraction of SR mechanism.

Soft growing robots also serve as personal assistants for people with disabilities or elderly individuals requiring daily task assistance. Their soft, flexible bodies facilitate safe lifting and carrying without risk of injury [9]. Soft pneumatic manipulators have been designed that can be slid under the human body to prevent bedsores. An eversion cantilever mechanism has been developed to support the human body posture effectively; the mechanism was combined with inflatable structures that had an inner skeleton structure with increased stiffness [10].

Although soft growing robots have demonstrated successful forward operation in various applications, reverse operation remains a challenge to be addressed. Achieving repeatability or reversibility requires successful "retraction" without buckling. Consequently, research on soft growing

Manuscript received: May 8, 2023; Revised September 13, 2023; Accepted November 22, 2023. This research was supported in part by a grant of the Korea Health Technology R&D Project through the Korea Health Industry Development Institute (KHIDI), funded by the Ministry of Health & Welfare, Republic of Korea (grant number : HI22C079600) and in part by the National Research Foundation of Korea under Grant NRF-2020R1A2C200416913. (*Corresponding author: Jee-Hwan Ryu.*)

[1]Nam Gyun Kim, and Dongoh Seo are with the Robotics Program, KAIST, 34141, Daejeon, Korea

[2]Shinwoo park, and Jee-Hwan Ryu are with the Department of Civil and Environmental Engineering, KAIST, 34141, Daejeon, Korea jhryu@kaist.ac.kr

robots' retraction mechanisms has been conducted. An inward movement mechanism for the tip material within the robot's body has been proposed [5], [11], [12] that enables retraction without buckling. This approach actuates the motor at the tip to retract only the tip material, avoiding buckling in the rest of the robot's body. However, using a rigid mechanism at the tip increases the robot's weight and limits its ability to navigate small spaces.

To address this limitation, researchers have focused on developing soft retraction mechanisms that preserve the inherent advantages of soft growing robots while achieving buckling-free retraction. Takahashi et al. employed water as the driving fluid for a soft growing robot, enabling buckling-free retraction [13]. The water's weight provided sufficient friction for the robot to resist the buckling moments. Additionally, an embedded compliant hollow mechanism inside the robot body helped prevent buckling while maintaining the robot's softness. However, using water as a driving fluid restricted the range of applications and increased the robot's weight. Heap et al. [14] proposed a soft retraction mechanism using air as the driving fluid, enabling the robot to retain most of its inherent advantages. However, this mechanism required an additional component for an inchworm-like movement at the tip, and the pneumatic control procedure complicated the robot control, resulting in slow retraction. Furthermore, the inchworm mechanism necessitated clamping of the inner material for retraction, impeding the utilization of the soft growing robot's inner channel.

This study introduces a novel retraction method, which enables buckling-free retraction without additional hardware or complex control sequences. The proposed mechanism is a soft growing robot that serves as its own retraction mechanism, hence called the self-retractable (SR) mechanism. The SR mechanism enables soft growing robots to retract faster and more simply. Its minimal design, consisting of only a retraction channel and sealing ring, facilitates easy integration with various tip mounts and steering mechanisms. Moreover, it maintains the benefits of soft growing robots without interfering with their inner channels during retraction.

The remainder of this paper is organized as follows. Section 2 outlines the SR mechanism concept. Section 3 details the working principles, design guidelines, prototyping, and fabrication of SR mechanisms. Section 4 presents experimental results and discusses the SR mechanism. Section 5 concludes the study.

II. Concept of SR Mechanism

Achieving retraction requires applying tail tension to a soft growing robot's inner material (tail). However, this tension can cause buckling moments along the robot body, particularly when the tail is biased toward one side. Increasing internal pressure to stiffen the robot body may help resist buckling, but it also increases tail tension, rendering it ineffective.

To eliminate adverse tail tension during retraction and generate an inversion force solely at the tip, we propose the SR mechanism. This mechanism successfully retracts a robot without buckling in both the straight and winding paths. It preserves most soft growing robots' inherent advantages and easily integrates with other mechanisms due to its simple structure. Additionally, the SR mechanism does not clamp the tail, allowing the inner channel to be utilized during retraction.

Fig. 1 illustrates the forward operation and retraction sequence of the SR mechanism. The SR mechanism comprises two main components: a retraction channel attached to the inside of the soft growing robot's body (purple in Fig. 1) and a sealing ring at the tip that prevents airflow from the retraction channel over the tip (red in Fig. 1). The sealing ring can be elastic or rigid, provided it effectively prevents airflow.

Fig. 1(a) demonstrates the growth of the soft growing robot with the SR mechanism. This growth process is identical to that of conventional soft growing robots. The uninflated retraction channel conforms to the body and does not interfere with the robot's everting process. Fig. 1(b) depicts the retraction process of the SR mechanism. To initiate retraction, the robot body's internal pressure P_B was first depressurized, and the retraction channel on the tail was pressurized with retraction pressure P_r. The inflated retraction channel then causes the sealing ring to move forward, propagating the inflation. As the sealing ring moves, the outer material naturally inverts into the tail section. Once the retraction channel's inflation fully propagates to the tip, the inner material along with the inflated retraction channel begins to push itself away from the robot tip and automatically retract the robot. Retraction of the SR mechanism can also be achieved by manually pulling the robot's tail at a rate that matched the sealing ring's movement speed. Importantly, the inflated retraction channel consistently straightens the flexible outer material, preventing scrunching during retraction.

In addition to preventing airflow during retraction, the sealing ring's placement at the tip offers several other advantages. It can reduce undesired friction between the inner channel and wires embedded in the inner channel. Embedded wires within the soft growing robot's inner channel were subjected to compression due to the pressure exerted by the robot body. To alleviate this compression and enable the wires to move freely, it is essential to apply equal pressure to both the inner channel and the main robot body. The placement of a sealing ring at the tip can effectively prevent airflow from the inner channel to the atmosphere, thereby facilitating the maintenance of equal pressure levels between the inner channel and the main robot body. Thus, a simple interlocking structure synchronizing the wire and sealing ring positions enables the soft growing robot to grow and retract properly, even with embedded sensor wires.

In addition to securing the inner channel, the sealing ring also enables the decoupling of tail tension from the body pressure, which determines the operation of the soft growing robot's growth and stopping. Particularly, the sealing ring prevents the tip from propagating until the internal pressure surpasses the pressure needed to move the sealing ring,

eliminating the need for manual tail lengthening control.

This paper details the implementation of the proposed SR mechanism in its original configuration, with the retraction channel located inside the robot body. However, the SR mechanism can function properly even in an everted configuration, where the retraction channel is positioned outside the robot body.

III. Working Principle and Design

This section explains the operating principle of the SR mechanism, along with design guidelines, prototyping, and fabrication details. All analyses were conducted under quasi-static conditions.

A. Issues on the Retraction of Soft Growing Robot

A conventional soft growing robot needs tension on the inner material (tail) and additional tension to invert the material at the tip for successful retraction [11]. The tail tension required for retraction in a conventional soft growing robot can be expressed as

$$T_T = \frac{1}{2}PA + F_I, \tag{1}$$

where A represents the cross-sectional area of the robot body, P denotes the internal pressure of the robot, and F_I refers to the additional tension required to invert the material at the tip. The value of F_I depends on the material properties, diameter, and thickness of the robot body.

However, tail tension T_T often leads to buckling of the soft growing robot during retraction. Specifically, when tail inclines towards one side of the curved robot body, it creates a buckling moment owing to the tail tension. While increasing the pressure on the robot body can enhance the outer body's stiffness and counteract this buckling moment, this is not a viable solution. As indicated in (1), tail tension T_T also increases as the robot body pressure rises.

B. Working Principle of the SR Mechanism

The operating principle of the SR mechanism differs significantly from conventional tail-pulling retraction methods. With the SR mechanism, the inflated retraction channel attached to the tail can be smoothly pulled without causing buckling, whereas the outer material continuously inverts due to a sealing ring at the tip that propagates forward with the inflation of the retraction channel. The SR mechanism applies the restoring moment of an inflated beam to the tail, rather than the robot's outer body, to resist buckling. As illustrated in Fig. 2(a), a basic inflated beam has a restoring moment that prevents buckling. However, conventional retraction mechanisms may result in buckling during the retraction process due to the larger buckling moment caused by the tail tension. In contrast, the proposed SR mechanism, which resembles a basic inflated beam, does not have any elements that generate unfavorable moments leading to buckling. This enables the robot to retract without encountering buckling issues while maintaining a restoring moment.

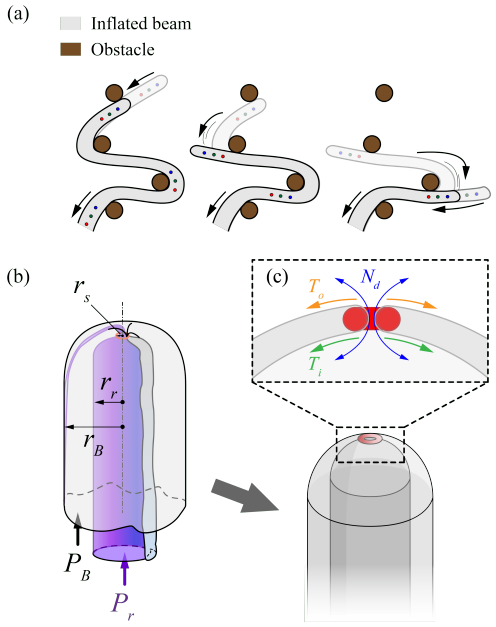

Fig. 2. Working principle of the SR mechanism. (a) Schematic depicting the pulling of an inflated beam within a constrained environment. (b) Parameters of the SR mechanism: sealing ring radius r_s, retraction channel radius r_r, robot body radius r_B, and applied pressures P_B, P_r. (c) Tension diagram: robot body wall tension T_o, retraction channel wall tension T_i, and tension related to the material deformation and friction of sealing ring N_d.

The most significant difference between the SR mechanism and the conventional retraction method lies in the fact that the force required to invert the material is no longer caused by tail tension. Fig. 2(b) illustrates the design parameters of the SR mechanism. r_s represents the radius of the sealing ring, r_r denotes the radius of the retraction channel, r_B is the radius of the robot body, P_B is the pressure applied to the robot's body, and P_r is the pressure applied to the retraction channel. As the retraction channel is attached to the robot body and inflates toward the sealing ring during the retraction process, the overall structure of the robot can be simplified, as shown in Fig. 2(c). The radial directional forces that occur at the robot's tip during retraction consist of the wall tension acting on the outer robot body T_o, wall tension acting on the retraction channel T_i, and tension related to the material deformation and friction of the sealing ring N_d, as illustrated in the enlarged dashed box in Fig. 2(c). For simplicity, we combined the expression for the tension related to material deformation and friction of the sealing ring into a single expression, N_d. The wall tension at the tip is expressed as:

$$T_o = P_B r_B \pi r_s, \;\; T_i = (P_r - P_B) r_r \pi r_s. \tag{2}$$

When the wall tension T_i of the retraction channel exceeds the combined wall tension of the outer robot body T_o and the tension arising from material deformation and friction of the sealing ring N_d, the material undergoes inversion. Therefore, for retraction to occur, the following inequality must be satisfied:

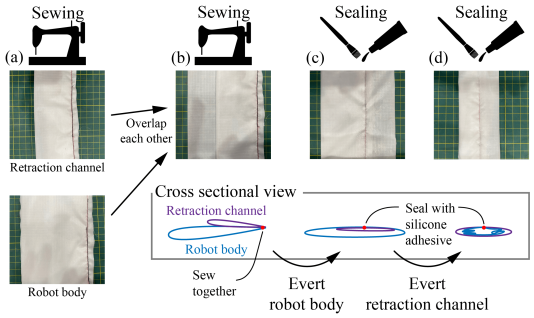

Fig. 3. Fabrication of SR mechanism.

$$T_i \geq T_o + N_d. \tag{3}$$

By substituting (2) into (3) and expressing it for pressure P_r applied to the retraction channel, the minimum pressure required for retraction can be formulated as

$$P_{r,min} = \frac{r_r + r_B}{r_r} P_B + \frac{N_d}{\pi r_s r_r}. \tag{4}$$

Notably, the robot can retract without the pressure of the outer body; in this case, the retraction pressure is used only to deform the material and overcome the friction of the sealing ring. Thus, the SR mechanism induces inversion of the material at the tip through wall tension generated by inflating the retraction channel.

C. Design Guidelines for SR mechanism

The ratio of the robot body diameter to that of the retraction channel diameter plays a critical role in designing the SR mechanism. A larger retraction channel diameter can facilitate stronger retraction at lower pressures, as demonstrated by (4). However, if the diameter is excessively large, jamming between the robot body and channel may occur, causing a sharp increase in retraction pressure. In this study, experimental findings supported a diameter ratio of 3:5 to achieve efficient retraction, whereas ratios greater than 4:5 led to inefficient retraction owing to material jamming.

While reducing the diameter of the retraction channel can further decrease tension owing to material deformation, high retraction pressure may be required. If the diameter is excessively small, generating the required inversion force may be challenging, even at high pressures, and the sealing ring may fail to seal airflow properly. Thus, when selecting the diameter ratio of the SR mechanism, it is recommended to use the largest diameter that does not cause jamming while considering the diameter of the sensor wire in the inner channel.

D. Fabrication Details and Prototyping

Fig. 3 displays the detailed fabrication process of the soft growing robot body with the retraction channel. The robot body and retraction channel were made of ripstop nylon fabric (60 μm, BOSUNG TEX), which has low friction and deformation force. The seams of the robot body and retraction channel were sewn together to prevent relative movement, as shown in Fig. 3(a–b). The seams were then sealed with a silicone adhesive to prevent air leakage, as shown in Fig. 3(c–d). An elastic toroidal latex rubber ring was used as the sealing ring.

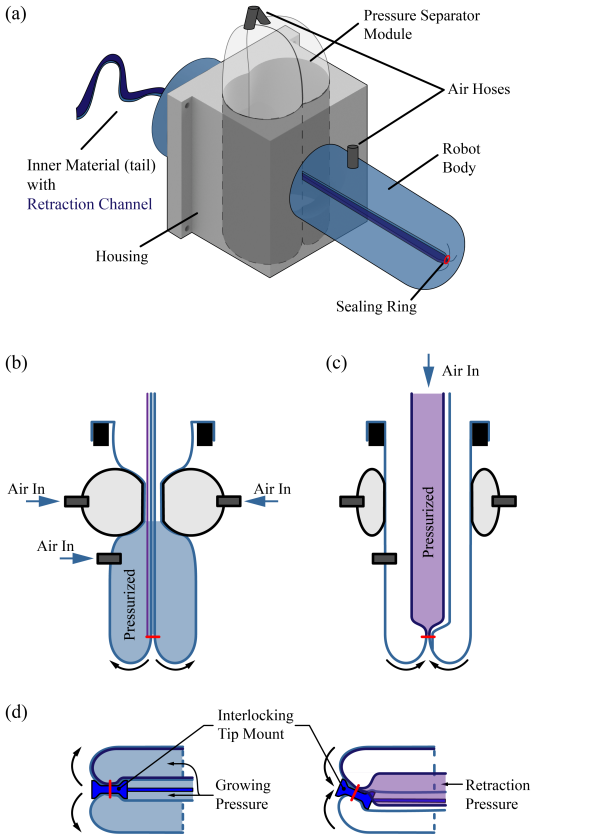

Fig. 4. Prototyping of the soft growing robot with SR mechanism. (a) Overall hardware of soft growing robot with SR mechanism. (b) Schematic diagram of growing phase. (c) Schematic diagram of retraction phase. (d) Interlocking tip mount embed in the soft growing robot with SR mechanism.

The remaining hardware components and their operational schematics are illustrated in Fig. 4. Fig. 4(a) depicts the overall hardware of the soft growing robot with the SR mechanism. Because the sealing ring effectively decouples the growth mechanism from tail tension, the need for a material feeding adjustment mechanism, such as a reel or rod, is eliminated, resulting in a simpler system. A pressure separator module is incorporated to maintain the pressure within the robot body and prevent it from being affected by ambient air pressure during expansion. This module also enabled a longer supply of materials. The operational schematics of the proposed mechanism for growth and retraction are illustrated in Figs. 4(b) and 4(c), respectively. To embed the wire in the inner channel, an interlocking mount can be used in conjunction with a sealing ring at the tip to synchronize the wire speed with the robot's body growth and retraction speed, as shown in Fig. 4(d).

IV. Experimental Evaluations

This section presents an experimental validation of the desired characteristics of the proposed SR mechanism and compares its performance with that of the conventional retraction method.

A. Growth Pressure

Before proceeding to the retraction experiments, we examined the eversion phase of the SR mechanism. We measured the minimum pressure required for growth with and without the SR mechanism. Robots equipped with a diameter of 63.6 mm and retraction channels of 38 mm diameter were utilized. A sealing ring, an elastic toroidal latex rubber, had an outer diameter of 5 mm and an inner diameter of 3 mm. A total length of 30 cm was everted, halving it to 15 cm, after which we gauged the least pressure required to initiate growth. While the conventional soft growing robot exhibited a growth pressure of 0.3 kPa, the SR mechanism required 1.2 kPa, representing mean values derived from five tests. Although the SR mechanism exhibited a marginally elevated growth pressure, the deviation was minimal and remained within functional limits.

B. Inversion Force

This subsection describes the measurement of the tip inversion force generated by the retraction pressure in the retraction channel to experimentally prove that the SR mechanism can generate a sufficient inversion force. This experimental validation also serves as a basis for designing the optimal diameter ratio between the robot body and retraction channel. Fig. 5(a) shows the experimental setup used to measure the inversion force of the SR mechanism. A load cell for measuring the inversion force was mounted on the ground, and a string extending from the load cell was attached to a fixed anchor sewn onto the inner material of the robot body. Two air hoses were attached to the ends of the retraction channel, one on the outer robot body and the other on the inner material, to release and apply pressure. The outer body of the robot was fixed to the ground to prevent any relevant movements during retraction and measure only the inversion force. Digital pressure sensors were embedded in the retraction channel, and the retraction pressure was logged simultaneously with the force measured by the load cell. The experimental values were measured after the robot began retracting because the anchor fixed to the tail was not initially tightened. Thus, the measured force indicated a residual inversion force after the material at the tip underwent deformation.

Fig. 5(b) shows the results of the inversion force experiment for three different diameter ratios. The experiments were conducted with robot bodies fabricated with a diameter of 63.6 mm. The solid red line corresponds to a 2:5 diameter ratio, the dashed green line to a 3:5 ratio, and the dotted blue line to a 4:5 ratio. Five tests were executed for each scenario. The actual experimental data are plotted in faded colors, and the fitted curves are shown in bright colors. The modeled wall tensions of the retraction channel, denoted as

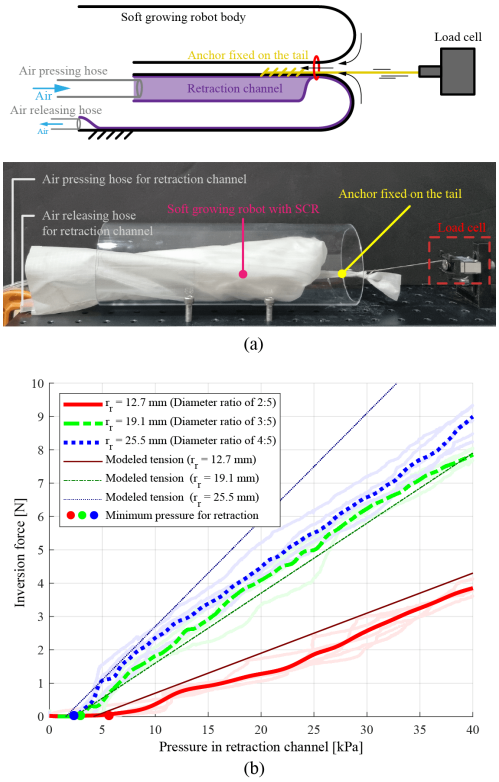

Fig. 5. Inversion force experiment. (a) Experimental setup. (b) Inversion force vs. pressure in retraction channel.

T_i in (2), correspond to the measured inversion forces are plotted in respective muted colors with thinner lines. The parameters used for these modeled tensions were ascertained in the experimental setup ($r_{s,2:5}$ = 3 mm, $r_{s,3:5}$ = 3.5 mm, $r_{s,4:5}$ = 4 mm), with N_d kept constant across all scenarios for optimal fit (N_d = 0.0005). The results suggest that a larger retraction channel diameter leads to greater inversion forces. Additionally, the data highlight that as the retraction channel diameter increases, the minimum pressures necessary for the inversion force to surmount both the sealing ring's friction and material deformation diminish. These pivotal pressures are denoted by the x-intercepts, which are marked with circular indicators.

For a diameter ratio of 4:5, the experimental data indicates a notably reduced force compared to the modeled tension, which is marginally greater than that for a 3:5 ratio. The decrease in force can be attributed to the jamming of the retraction channel with a 4:5 diameter, when combined with the inflated retraction channel and the hose containing the pressure sensor. This jamming results in a loss of the force that acts as the inversion force. A discrepancy was observed between the modeled wall tensions and the observed inversion forces, particularly regarding the minimum pressure essential for retraction. This variance emerges because the volume of material passing through the sealing rings increases with the increase of the retraction channel diameter. This increase influences the N_d term, which was set to a constant value in the modeled wall tensions. Consequently,

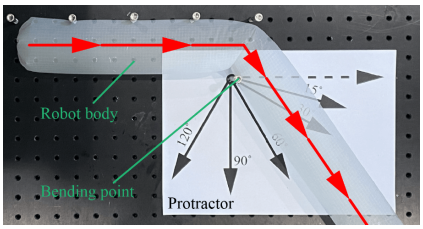

Fig. 6. Setup for success rate of retraction experiment.

TABLE I
SUCCESS RATE OF RETRACTION

Bent angle [°]	15	30	60	90	120
Conventional tail pulling	40	0	0	0	0
Proposed SR mechanism	100	100	100	100	70

even with a larger retraction channel diameter, the retraction pressure does not decrease enough to counter the sealing ring's resistance force. In summary, an excessively large diameter can cause material jamming without reducing the pressure required for triggering the retraction, resulting in high pressure that is insufficient to overcome the resistance force of the sealing ring. Additionally, if the gap the robot needs to navigate is narrower than the inflated retraction channel, the retraction mechanism might be hindered. This is due to the inflated retraction channel getting caught in the gap, thereby elevating the tension in the inner material essential for retraction, even if it is unrelated to buckling. Therefore, employing a diameter ratio of 3:5 is recommended to generate a substantial inversion force at relatively lower pressures, while minimizing the potential for material blockages and undue tension stemming from the size of the inflated retraction channel.

C. Success Rate of Retraction

We investigated the success rate of retraction across varying bent angles to quantify the performance of the SR mechanism in comparison to the conventional tail-pulling method. Fig. 6 shows the experimental setup. Both methods were tested with an identical robot body diameter of 63.6 mm to ensure consistent comparison, and the proposed method maintained a diameter ratio of 3:5. In the conventional tail-pulling approach, a minimum pressure of 4 kPa was employed to inflate the robot's body, preventing it from collapsing during retraction. In contrast, the SR mechanism required no such body inflation; only the retraction channel was inflated to 7 kPa, the lowest pressure ensuring reliable retraction across all experimental settings. Each scenario underwent ten trials. The retraction velocity was maintained at 7 cm/s for both methods, and any buckling surpassing 30 degrees was deemed a failure.

Table I reveals that the conventional tail-pulling method had a success rate of just 40% at a 15-degree angle, which then plummeted to zero for all subsequent angles tested. On the other hand, the SR mechanism consistently showcased a 100% success rate for angles up to 90 degrees. Beyond this, the SR mechanism did face occasional setbacks, especially when the sealing ring attempted to revert the wrinkled material, subsequently inhibiting further inversion.

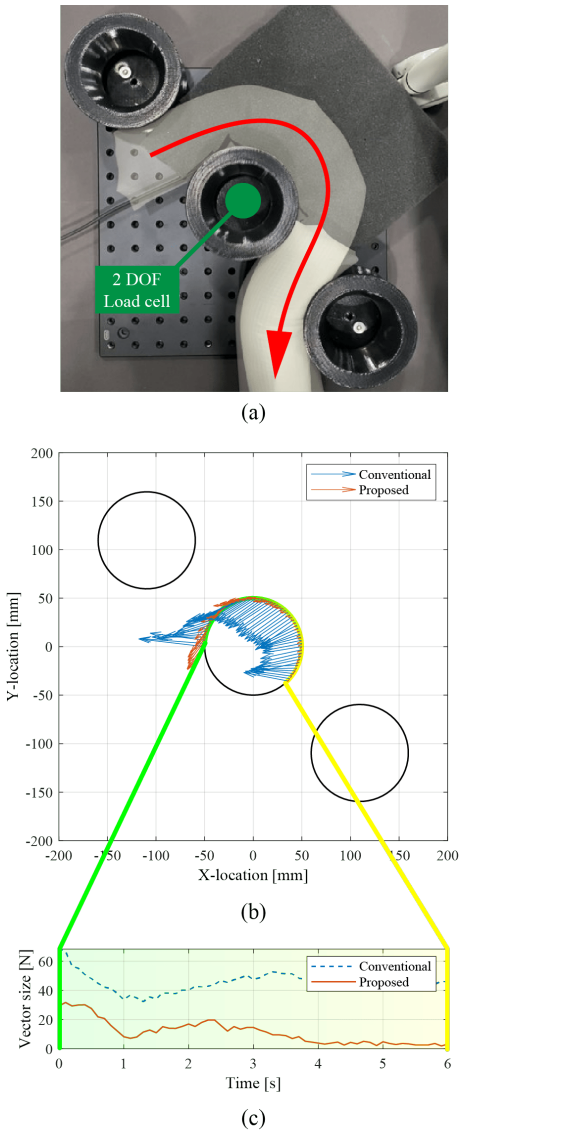

Fig. 7. Obstacle interaction force experiment. (a) Experimental setup. (b) Vector illustration of interaction force during retraction. (c) Magnitude of the interaction force during retraction.

D. Obstacle Interaction Force

This subsection presents a comparative analysis of the interaction forces encountered when negotiating obstacles during the retraction process. We compared the conventional tail-pulling technique with the SR mechanism. For this study, robot conditions remained consistent with those detailed in Section IV-C. Fig. 7(a) shows the experimental setup used to measure the obstacle interaction force. Both robots were retracted at an identical speed of 7 cm/s, as indicated by the red arrow in Fig. 7(a). We employed a 2-DOF load cell to monitor the interaction force exerted by the central obstacle during the retraction phase. This load cell was strategically positioned at the center cylinder to primarily record the

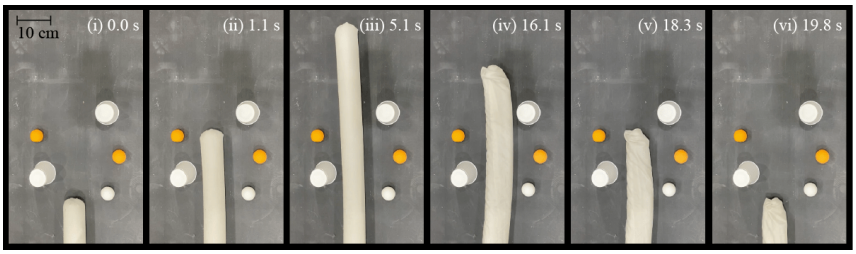

Fig. 8. Growth and retraction of the soft growing robot with SR mechanism.

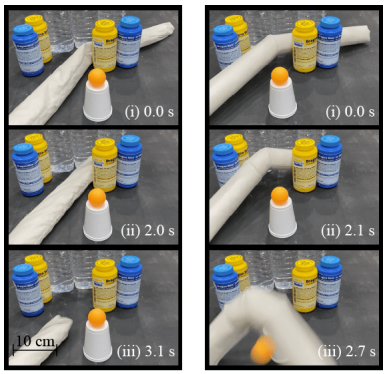

Fig. 9. Retraction demonstration of soft growing robot (a) Proposed retraction. (b) Conventional retraction.

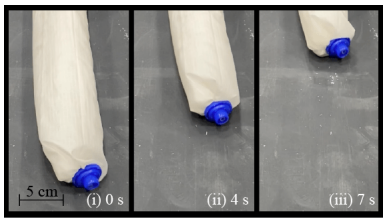

Fig. 10. Retraction demonstration of SR mechanism with the secured inner channel and tip mount.

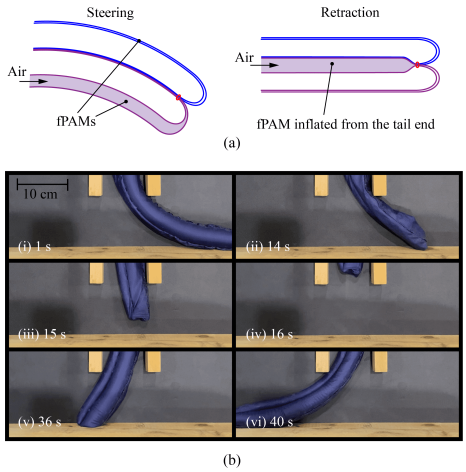

Fig. 11. (a) Schematic representation of the SR mechanism, which employs a pneumatic actuator as the retraction channel. (b) Demonstration of steering and retraction capabilities.

2D planar buckling force which acts inwardly, targeting the center cylinder within the robot's curvature. As shown in Fig. 7(b), the conventional tail-pulling method produced an undesirably high interaction force because the robot body had to be inflated with sufficient pressure to prevent scrunching. However, the proposed method requires the inflation of only the retraction channel, which has a smaller diameter and a lower restoring moment. Therefore, the proposed mechanism exerts a significantly lower interaction force on obstacles. The direction of the initial restoring force varies due to the robot's pose, which is influenced by the inflation of the retraction channel and the robot body. Additionally, owing to the buckling problem, the conventional method continues to exert a high interaction force even after passing the first obstacle. However, the proposed mechanism exerts a significantly lower interaction force after passing through the first obstacle. Fig. 7(c) shows the magnitude of the interaction force over time. The conventional retraction mechanism exerted approximately twice the interaction force of the proposed mechanism before passing the first obstacle, and after passing the first obstacle, the interaction force was even higher. Notably, after passing the center obstacle, the conventional retraction method failed to retract owing to complete collapse caused by buckling, whereas the proposed mechanism successfully retracted without any issues.

E. Demonstrations

This subsection presents four distinct scenarios to demonstrate the capabilities of the proposed SR mechanism. Based on the investigations in Section IV-B, we designed all robots with a diameter ratio of 3:5, which showed the best performance. To achieve optimal performance of the SR mechanism, we released the pressure on the main body of the robot during retraction to generate high inversion forces. Four demonstrations were conducted. The first demonstration involved growing and retracting a messy terrain in a straight configuration. As depicted in Fig. 8, the soft growing robot grew straight with the SR mechanism and retracted along the grown path, thanks to the buckling-free retraction capability of the SR mechanism. Consequently, the robot could retract successfully without disturbing the obstacles.

The second demonstration involved retracting the robots in a bent configuration using the conventional tail-pulling method and proposed SR mechanism, as shown in Fig. 9. The robot that used the conventional tail-pulling method was

operated at a pressure that did not cause wrinkles in the straight portion of the robot during tail pulling. As depicted in Fig. 9(a), the robot equipped with the SR mechanism retracted effectively without any buckling issues. In contrast, Fig. 9(b) shows that the robot utilizing the conventional tail-pulling method applied force to the obstacles during retraction, resulting in severe buckling problems that ultimately led to environmental damage.

The third demonstration of the SR mechanism showcases its potential for tasks requiring wired sensors at the tip by securing the inner channel with a tip mount during retraction, as shown in Fig. 10. The tip mount, which has a similar diameter to the retraction channel, was assembled using the interlocking structure described in Section III-D. Despite the increased pressure for retraction due to the interlocking mechanism, the robot successfully retracted with the tip mount and wires inside the inner channel. While a higher retraction pressure may cause inefficient retraction due to airflow leakage through the sealing ring, this does not affect the environment near the robot since the pressure in the retraction channel is released at the opening attached to the base and does not leak from the robot body.

In a final demonstration, the SR mechanism showcased its adaptability by seamlessly integrating with a steering actuator. As discussed in Section II, the SR mechanism functions properly even in an everted layout, wherein the retraction channel exists externally to the robot body, mirroring pneumatic steering actuators. Therefore, fabric pneumatic artificial muscles (fPAMs) were directly utilized as the retraction channel in this demo. These fPAMs were inflated from the tail end to facilitate retraction. As illustrated in Fig. 11, the robot adeptly maneuvered through its environment while achieving buckling-free retraction. Such a demonstration emphasizes the versatility and modularity of the SR mechanism, suggesting its potential inclusion in more advanced robotic systems that require both consistent retraction and the complex navigation enabled by steering actuators.

V. Conclusion

In this study, we introduced the self-retractable (SR) mechanism, a pioneering retraction approach that ensures buckling-free retraction without necessitating supplementary rigid components. This proposed mechanism stands out in its efficiency and reliability, demanding minimal alterations to the existing robot design. Leveraging a single pneumatic channel, the SR mechanism retains the intrinsic adaptability characteristic of soft growing robots. Our analytical and experimental evaluations confirmed the mechanism's efficacy, demonstrating its capability to retract the soft growing robot in diverse configurations, including straight and bent states, without encountering buckling challenges. Moreover, by securing the inner channel with a tip mount and integrating it with steering actuators, we showed the practical viability of our proposed retraction methodology.

This advancement holds substantial promise for the field of soft growing robots. By offering buckling-free retraction without the intricacies of rigid systems, it can catalyze the inception of innovative applications in areas necessitating wired sensors and tools deployed through the inner channel for iterative tasks. Consequently, our findings present a promising trajectory for the development of more advanced and practical soft robotic technologies. In future research, we intend to further investigate optimizations of the mechanism, particularly focusing on the robot base design for efficient material stacking and determining the optimal size of sealing rings. Additionally, we aim to explore the mechanism's adaptability in more complex environments, using various types of soft growing robots.

References

[1] D. Mishima, T. Aoki, and S. Hirose, "Development of pneumatically controlled expandable arm for search in the environment with tight access," in *Field and Service Robotics*, pp. 509–518, Springer, 2003.

[2] E. W. Hawkes, L. H. Blumenschein, J. D. Greer, and A. M. Okamura, "A soft robot that navigates its environment through growth," *Science Robotics*, vol. 2, no. 8, p. eaan3028, 2017.

[3] H. Tsukagoshi, N. Arai, I. Kiryu, and A. Kitagawa, "Smooth creeping actuator by tip growth movement aiming for search and rescue operation," in *2011 IEEE international conference on robotics and automation*, pp. 1720–1725, IEEE, 2011.

[4] M. M. Coad, L. H. Blumenschein, S. Cutler, J. A. R. Zepeda, N. D. Naclerio, H. El-Hussieny, U. Mehmood, J.-H. Ryu, E. W. Hawkes, and A. M. Okamura, "Vine robots: Design, teleoperation, and deployment for navigation and exploration," *IEEE Robotics & Automation Magazine*, vol. 27, no. 3, pp. 120–132, 2019.

[5] J. Luong, P. Glick, A. Ong, M. S. deVries, S. Sandin, E. W. Hawkes, and M. T. Tolley, "Eversion and retraction of a soft robot towards the exploration of coral reefs," in *2019 2nd IEEE International Conference on Soft Robotics (RoboSoft)*, pp. 801–807, IEEE, 2019.

[6] P. A. der Maur, B. Djambazi, Y. Haberthür, P. Hörmann, A. Kübler, M. Lustenberger, S. Sigrist, O. Vigen, J. Förster, F. Achermann, *et al.*, "Roboa: Construction and evaluation of a steerable vine robot for search and rescue applications," in *2021 IEEE 4th International Conference on Soft Robotics (RoboSoft)*, pp. 15–20, IEEE, 2021.

[7] P. Slade, A. Gruebele, Z. Hammond, M. Raitor, A. M. Okamura, and E. W. Hawkes, "Design of a soft catheter for low-force and constrained surgery," in *2017 IEEE/RSJ International Conference on Intelligent Robots and Systems (IROS)*, pp. 174–180, IEEE, 2017.

[8] P. Berthet-Rayne, S. H. Sadati, G. Petrou, N. Patel, S. Giannarou, D. R. Leff, and C. Bergeles, "Mammobot: A miniature steerable soft growing robot for early breast cancer detection," *IEEE Robotics and Automation Letters*, vol. 6, no. 3, pp. 5056–5063, 2021.

[9] T. Nakamura and H. Tsukagoshi, "Soft pneumatic manipulator capable of sliding under the human body and its application to preventing bedsores," in *2018 IEEE/ASME International Conference on Advanced Intelligent Mechatronics (AIM)*, pp. 956–961, IEEE, 2018.

[10] T. Takahashi, M. Watanabe, K. Abe, K. Tadakuma, N. Saiki, M. Konyo, and S. Tadokoro, "Inflated bendable eversion cantilever mechanism with inner skeleton for increased stiffness," *IEEE Robotics and Automation Letters*, vol. 8, no. 1, pp. 168–175, 2022.

[11] M. M. Coad, R. P. Thomasson, L. H. Blumenschein, N. S. Usevitch, E. W. Hawkes, and A. M. Okamura, "Retraction of soft growing robots without buckling," *IEEE Robotics and Automation Letters*, vol. 5, no. 2, pp. 2115–2122, 2020.

[12] S.-G. Jeong, M. M. Coad, L. H. Blumenschein, M. Luo, U. Mehmood, J. H. Kim, A. M. Okamura, and J.-H. Ryu, "A tip mount for transporting sensors and tools using soft growing robots," in *2020 IEEE/RSJ International Conference on Intelligent Robots and Systems (IROS)*, pp. 8781–8788, IEEE, 2020.

[13] T. Takahashi, M. Watanabe, K. Tadakuma, M. Konyo, and S. Tadokoro, "Retraction mechanism of soft torus robot with a hydrostatic skeleton," *IEEE Robotics and Automation Letters*, vol. 5, no. 4, pp. 6900–6907, 2020.

[14] W. E. Heap, N. D. Naclerio, M. M. Coad, S.-G. Jeong, and E. W. Hawkes, "Soft retraction device and internal camera mount for everting vine robots," in *2021 IEEE/RSJ International Conference on Intelligent Robots and Systems (IROS)*, pp. 4982–4988, IEEE, 2021.